POLITECNICO DI TORINO
Repository ISTITUZIONALE

Impact of rice bran wax composition and oleogelation conditions on the structural stability of sunflower oil-based oleogels

Original
Impact of rice bran wax composition and oleogelation conditions on the structural stability of sunflower oil-based oleogels / Candela, D., Brykczynski, H., Fiore, C., Flöter, E., Simone, E.. - In: FOOD STRUCTURE. - ISSN 2213-3291. - 50:(2026), pp. 1-15. [10.1016/j.foostr.2026.100568]

Availability:
This version is available at: 11583/3016824 since: 2026-10-20T10:11:08Z

Publisher:
Elsevier

Published
DOI:10.1016/j.foostr.2026.100568

Terms of use:

This article is made available under terms and conditions as specified in the corresponding bibliographic description in the repository

Publisher copyright

(Article begins on next page)

18 November 2026

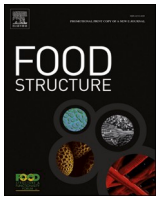
Food Structure 50 (2026) 100568



Contents lists available at ScienceDirect

Food Structure

journal homepage: www.elsevier.com/locate/foostr



Impact of rice bran wax composition and oleogelation conditions on the structural stability of sunflower oil-based oleogels

Danilo Candela [a], Henriette Brykczynski [b], Cecilia Fiore [a], Eckhard Flöter [b], Elena Simone [a,*]

[a] Department of Applied Science and Technology (DISAT), Politecnico di Torino, Torino, Italy
[b] Department of Food Process Engineering, Technische Universität Berlin, Berlin, Germany

ARTICLE INFO

Keywords:
Rice bran wax
Oleogelation process
Fat replacement
Oleogels

ABSTRACT

The growing demand for healthier ingredients has driven research toward innovative systems, such as oleogels, which can provide nutritional benefits without compromising food texture and mouthfeel. Among various structuring agents, rice bran wax (RBX) is a promising candidate for creating three-dimensional networks in liquid vegetable oils. However, the functional success of these systems is heavily dependent on wax composition and processing conditions. This study investigates the impact of RBX compositional profile and oleogelation conditions on the structural stability of sunflower oil-based oleogels. A laboratory-extracted RBX (obtained via an optimised isolation protocol) was compared with two commercial alternatives to evaluate the possible influence of interfering compounds on microstructural assembly. Results show that the compositional profile of the laboratory-purified RBX promotes highly cohesive inter-crystalline interactions, yielding a robust and continuous solid matrix even at low concentration (1%wt) depending on the process conditions. Conversely, the application of mechanical stirring during the oleogelation phase was found to hinder the development of a continuous solid network, promoting the formation of aggregates that led to notable oil separation during storage. Under these dynamic conditions, minor components present in commercial waxes appeared to partially mitigate this aggregation, indicating a clear trade-off between compositional homogeneity and resilience against mechanical stress. These findings demonstrate that high-performance oleogels can be achieved by optimising both wax isolation protocols and environmental conditions during oleogelation. This research provides fundamental insights for future research aimed at incorporating chemically uniform RBX oleogels into complex food matrices as a sustainable alternative to saturated fats, contributing to the development of improved lipid-based food products.

1. Introduction

In recent years, increasing attention has been paid to what people eat and how diet might affect our health and the environment (Springmann et al., 2018; Webb et al., 2023). Over the last few decades, in fact, significant correlations have been observed in developed nations between non-optimal dietary patterns and the rising incidence of chronic diseases, most notably cardiovascular and oncological pathologies (Hull et al., 2025; P. Wang et al., 2023). The emergence of these pathologies is frequently attributed to the high consumption of ultra-processed foods characterised by elevated saturated fat content; such dietary profiles result in a caloric surplus, which might be a primary driver for these conditions (De Souza et al., 2015; Hull et al., 2025; Schnabel et al., 2018; Stepanenko, 2025). To mitigate these concerns, novel classes of colloidal lipid-based systems have been engineered and designed to optimise nutritional profiles without compromising functional properties. Among these systems, oleogels represents an extensively investigated class due to their diverse functional applications and the vast landscape of potential formulations involving distinct lipid phases and gelling agents (Flores-García et al., 2023; Sivakanthan et al., 2022; Z. Wang et al., 2023). Typically, these structuring agents are blended and incorporated into the liquid oil phase, favouring the development of a three-dimensional network that provides structural integrity to the starting liquid oil (Sivakanthan et al., 2022; Zhang et al., 2023). Among the most extensively studied oleogelators, two main classes are generally distinguished: low-molecular (LMWOs) and high-molecular (HMWOs)

* Corresponding author.
E-mail address: elena.simone@polito.it (E. Simone).

https://doi.org/10.1016/j.foostr.2026.100568
Received 23 July 2026; Received in revised form 28 September 2026; Accepted 29 September 2026
Available online 30 September 2026
2213-3291/© 2026 The Author(s). Published by Elsevier Ltd. This is an open access article under the CC BY license (http://creativecommons.org/licenses/by/4.0/).

weight oleogelators (Sivakanthan et al., 2022; Z. Wang et al., 2023). The former category comprises crystalline particles, such as natural waxes, fatty acids, and mono-, di-, or triglycerides, whereas the latter consists of polymers like carbohydrates and proteins. Research has predominantly focused on LMWOs, as their direct solubility in the lipid phase allows for the formation of stable oleogels even at minimal concentrations (Cerqueira et al., 2017; Kavya et al., 2024; Martins et al., 2022).

Natural waxes are extensively employed oleogelators because they are frequently obtained as agricultural by-products (Abe et al., 2025; Tan et al., 2023; Thakur et al., 2023). Integrating these materials back into the production chain enhances environmental sustainability and aligns with circular economy principles (Esposito et al., 2020; Korhonen et al., 2018). Several types of waxes are used in the preparation of oleogels. The most common ones include beeswax, carnauba wax, candelilla wax, sunflower wax, and rice bran wax (RBX) (Dimakopoulou-Papazoglou et al., 2025; Doan et al., 2015; Doan, Tavernier, et al., 2017; Sivakanthan et al., 2022). While beeswax comes from an animal source (which generally raises ethical concerns about the exploitation of bees (Loiacono et al., 2025)), the other types come from plant sources, making them more sustainable and widely accepted alternatives. From a chemical perspective, waxes are heterogeneous substances primarily characterised by long-chain esters derived from the esterification of long-chain fatty acids and alcohols (Hargrove et al., 2004; Sivakanthan et al., 2022; Tavernier et al., 2017). While wax esters constitute the majority of wax composition, these materials also incorporate a diverse range of minor constituents, including n-alkanes, sterol esters, and pentacyclic triterpenoid derivatives (Sivakanthan et al., 2022). Such chemical heterogeneity is reflected in their thermal properties, with melting ranges varying from 30°C to 90°C. This highlights the importance of the extraction and purification processes employed to refine the wax and tailor its properties for specific applications (Athukorala et al., 2009). Although these additional extraction and refining steps inevitably increase raw material processing costs, the high structuring efficiency of purified waxes compensates for this drawback by enabling stable gelation at very low concentrations (typically 0.5–3 wt%). As a result, the overall cost of the final oleogel formulation remains economically competitive against traditional fractionated fats, representing a viable and scalable route for saturated fat replacement in industrial applications (Scharfe & Flöter, 2020).

The combination of thermal and structural features, arising from the specific chemical composition of the wax oleogelator, has a significant impact on the properties of the resulting oleogel (Blake et al., 2014; Holey et al., 2021). As an example, waxes containing high amounts of wax esters (as is the case of sunflower wax) deliver large, needle-shaped crystals during the oleogelation process, which are highly effective at trapping the liquid phase (Doan, Tavernier, et al., 2017; Shi et al., 2021). The final result is a firm gel that remains stable even at high temperatures and shows better resistance when subjected to mechanical stresses compared to waxes with low content of esters.

RBX represents an ideal case study to investigate these structure-function relationships. Rice bran is an abundant agricultural secondary product coming from the rice milling process. To valorise this residue, rice bran oil can be extracted and commercialised after being refined. RBX is obtained during the dewaxing step of this refining process, and it is mainly composed of wax esters, but also of some other components such as fatty acids, and fatty alcohols. The use of RBX as an oil-gelling agent has been reported in different studies involving several types of vegetable oils (Bayomy & Almasoudi, 2025; Dassanayake et al., 2009, 2011; Sahu et al., 2020; N. Wang et al., 2021). In most cases, RBX has proven to be a compound capable of forming stable crystalline networks at low concentrations. In the work of Wijarnprecha et al., 2018, RBX (ranging between 0.5%wt and 25%wt) was blended with rice bran oil and it was found that the 0.5%wt concentration can produce a stable structure when stored at a temperature below 15°C (Wijarnprecha et al., 2018). When prepared with higher RBX concentrations, the structural, mechanical, and thermal properties of the relative oleogels were found to improve as a function of the network of the interlinked needle crystals formed. A similar behaviour was found also by N. Wang et al., 2021, who observed that, when structuring rice bran oil, a minimum concentration of 7%wt of RBX was necessary to obtain an oleogel at 20 °C (N. Wang et al., 2021). This significant discrepancy in the minimum gelling concentrations reported (0.5%wt (Wijarnprecha et al., 2018) and 7%wt (N. Wang et al., 2021)) can be attributed to some variations in the composition and laboratory-scale isolation methods of the employed waxes. It is possible that the specific extraction protocol used in the work of N. Wang et al., 2021 led to a higher degree of minor components compared to commercial standards. Such compounds can hinder the formation of the crystalline network, requiring a higher wax content to achieve a stable oleogel. Another inconsistent result was reported by Doan et al., 2015 (Doan et al., 2015). They observed a minimum RBX concentration of 5%wt in rice bran oil and justified this phenomenon by pointing out a weaker interaction between the wax and RBO. This weak interaction limits the formation of a tight crystal network, causing the RBX to crystallise into large dendritic structures rather than the highly efficient, needle-like or fibrous networks formed in other vegetable oils such as olive and salad oil. The effect of the composition of the wax used on the properties of the resulting oleogels has been extensively studied by Wettlaufer et al., 2021 (Wettlaufer et al., 2021). In their work, wax esters are highlighted as the primary drivers of oleogelation due to their linear structure, which promotes rapid gel-sol transitions and low undercooling. Consequently, waxes with high ester content, such as sunflower wax and RBX, exhibit enhanced structuring efficiency. Nonetheless, despite their similar wax ester content, sunflower wax presents a narrower ester distribution, promoting the formation of highly interconnected needle-like crystals resulting in more stable oleogels compared to RBX. Conversely, the presence of high proportions of non-ester components significantly impairs gel performance. For instance, high concentrations of free fatty alcohols (e.g. in carnauba wax (Dassanayake et al., 2009)) or free fatty acids and hydrocarbons (e.g. in beeswax (Doan, To, et al., 2017)) induce complex, multi-peak thermal transitions and severe undercooling, ultimately disadvantaging the formation of a cohesive and stable crystalline network. These compositional interferences become even more critical when oleogels are incorporated into real food matrices (Scharfe & Flöter, 2020). The co-existence of other common food ingredients, such as water droplets in emulsified systems, surfactants like lecithin (Okuro et al., 2018), or co-crystallising lipids (Blake et al., 2014), can significantly alter wax crystallisation kinetics and crystal habit and polymorphism, often leading to network destabilisation. Consequently, utilising an unrefined wax with intrinsic chemical impurities can amplify these matrix-induced disruptions, making structural behaviour highly unpredictable (Scharfe & Flöter, 2020). In contrast, starting with a highly purified wax ensures a more predictable, resilient crystalline structure capable of mitigating external matrix interferences while maintaining low the minimum gelling concentrations.

Effective isolation of RBX requires protocols that prioritise both purity and recovery. Refined extraction steps are necessary to prevent the carryover of contaminants, which, as previously noted, can significantly affect the wax's performance in oleogel systems. In this regard, our previous work (Candela et al., 2025) proposed five different strategies for isolating RBX from rice bran butter. Although all five processes studied resulted in the isolation of highly pure waxes, only one strategy (referred to in the paper as “Process #2”) achieved the best results in terms of extraction yield. The resulting material was characterised in terms of its thermal and structural properties, while the sustainability of the extraction process was evaluated using Life Cycle Assessment (LCA) (Candela et al., 2025). Nevertheless, the characterisation of the chemical composition of the obtained wax was not performed and its potential use as an oil-gelling agent was never tested.

The aim of this study is to fill these gaps by characterising the RBX obtained from Process #2 (hereinafter referred to as RBXP) from a chemical perspective in comparison with two commercial RBXs. To do

so, LC-ELSD provided quantitative, carbon-number-resolved information on the aliphatic composition of the waxes, focusing on the wax ester fraction. FTIR was employed, aiming to identify differences in the minor component fractions. The RBXs' structuring abilities as oleogelator were compared by forming oleogels with sunflower oil (SO) at different concentrations. Results suggest that a minimum quantity of 1%wt of RBXP is necessary to obtain a stable oleogel at room temperature. It was also found that a stable crystal network can be formed with RBXP only if the cooling step during oleogel formation is kept at static conditions without any use of stirring. Finally, thermal and structural analyses confirmed that the functional behaviour of the resulting oleogels is strictly related to the nature of the wax used. These findings highlight that the success of the oleogelation process is strictly governed by the compositional profile of the structuring agent. Modulating the wax composition alters the delicate balance between the self-affinity of wax molecules, the establishment of a continuous structural network, and the tendency of such network to generate agglomerates under mechanical stress, which is a critical requirement for the reliable formulation of lipid-based food products.

2. Materials and methods

2.1. Materials

Commercial RBXs were compared with a laboratory-scale isolated RBX obtained according to our previously developed process (Candela et al., 2025). The RBX used was recovered from a rice bran butter matrix obtained through supercritical CO_2 extraction. Rice bran butter was then subjected to a series of melting, solvent additions, centrifugations, and a final vacuum filtration. Although the Life Cycle Assessment showed that using ethanol for the purification offers a better balance between the yield of the extracted wax and the environmental impact, the solvent employed for all the purification steps was decided to be 2-propanol (99.8% pure, Sigma-Aldrich) [40]. The reason lies in the fact that the samples extracted with 2-propanol exhibited more uniform thermal properties, suggesting that the extracted RBXP might be more uniform in terms of chemical composition. RBXA was kindly provided by TH.C. TROMM GmbH (Cologne, Germany) and RBXB was kindly provided by KAHL GmbH & Co. KG (Trittau, Germany). Oleogels were formed by blending the RBXs with sunflower oil (SO) purchased from a local market (Pam Panorama, Italy). Acetonitrile (ACN), HPLC-grade water (H_2O), and HPLC-grade ethanol (EtOH) were purchased from VWR. HPLC-grade Methyl-tertiary-butyl-ether (MTBE) and tri-fluoroacetic acid were purchased from Carl Roth. As an external standard to compensate for retention time shifts, a mixture of 13 standards of high purity was used, see Table S1 of Supporting Information.

2.2. RBX chemical characterisation

2.2.1. Liquid chromatography

Native wax composition was analysed according to a single-step LC-ELSD method, see (Brykczynski et al., 2026). Standard stock solutions (125 μg/mL per analyte) were prepared in volumetric flasks by adding 99% (v/v) MTBE and 1% (v/v) EtOH to the respective wax. After dissolution at 35 °C, samples were cooled to ambient temperature, filtered through hydrophobic PTFE filters (0.2 μm pore size), and transferred to injection vials with a PTFE septum.

All measurements were performed on an Agilent 1260 Infinity II quaternary system (Agilent Technologies Inc., Waldbronn, Germany) including a G7111B quaternary pump (Agilent, Waldbronn, Germany), G7129C vial sampler with 100 μL injection loop (injection volume 10 μL) (Agilent, Waldbronn, Germany), 1260 Infinity II multicolumn thermostat (Agilent, Waldbronn, Germany) and 1290 II Infinity ELSD (Agilent, Waldbronn, Germany). The nebuliser temperature was 35 °C, the evaporator temperature 90 °C at a nitrogen flow of 1.2 L/min. Nitrogen was produced by a Solaris 10 generator (Peak Scientific Instruments GmbH, Düren, Germany). An OTU MonoKala C18 column without endcapping (105 Å, 5 μm, 250 ×4.6 mm), protected by a guard column of the same specifications (10 ×4.6 mm), was employed at 30 °C (both columns: AppliChrom GmbH, Oranienburg, Germany). Two eluents were used at a flowrate of 1 mL/min: Eluent A consisted of 99.495% (v/v) CAN, 0.5% (v/v) H2O, and 0.005% (v/v) TFA. Eluent B consisted of 98.995% (v/v) MTBE, 0.5% (v/v) EtOH and 0.005% (v/v) TFA. The employed gradient is given in Table S2 of Supporting Information. Between two runs, a flushing run was performed to ensure cleaning and conditioning of the columns. Measurements were performed in triplicate. Instrument control was performed with the manufacturer's software OpenLab CDS 2.4, and data analysis was performed following the workflow of Brykczynski et al. (2026).

Wax components were quantified as relative mass percentages within the resolved fraction. This was necessary due to the inherent non-linear response of the ELSD and day-to-day signal variability (see (Brykczynski et al., 2026)). Method validation using standard mixtures established that the upper linearity/detector limit ranged between 62.5 and 125 μg/mL, while lower limits of quantification (LOQ) varied by carbon number (with up to 5 μg/mL for short-chain species such as FA18, FaOH20–24, HC27, and WE24). To account for the highest LOQ among minor components and ensure robust relative integration, a conservative operational reporting limit of 5 m% was applied for individual component reporting.

2.2.2. Fourier-transform infra-red spectroscopy (FTIR)

To record FTIR spectra of the solid wax samples, no further sample preparation was required. Spectra were recorded with a diamond attenuated total reflection (ATR) on a Lyza 7000 FT-IR spectrometer (Anton Paar, Graz, Austria), equipped with an IR source, a KBr-beamsplitter, and a DLaTGS (deuterated L-alanine triglycine sulphate) KBr-detector. All samples were measured in triplicate in the spectral range from 5000 to 500 cm^{-1} using 32 scans at a resolution of 2 cm^{-1}. A background spectrum was acquired after every ten measurements. Data processing was carried out using MATLAB R2021b. For comparability, spectra were shifted to 100% extinction in the region from 4000 to 5000 cm^{-1} and normalised to the band at 2919 cm^{-1}.

2.3. Oleogelation process

The oleogelation process was conducted by mixing the different RBXs with SO in different proportions. Oleogels were prepared in duplicate. The concentrations of RBXP in SO tested were 0.5%wt, 1%wt, 2%wt, 3%wt, 5%wt, and 10%wt in a total weight of 1000 mg (corresponding to a filling volume of approximately 1.1 mL); RBXA and RBXB were only tested at 1%wt and 5%wt concentrations. Samples were prepared in 2 mL clear glass vials using the Crystal 16 multi-reactor apparatus (Technobis, Netherlands). Agitation was provided using a top-driven, magnetically driven overhead hook-impeller (diameter: 7 mm, rod length: 17 mm, total impeller length: 23 mm). The impeller was positioned perpendicularly to the vial's vertical axis. With this equipment, 16 samples at a time can be prepared, controlling temperature profiles and stirring rates using the hook-Hastelloy stirring impellers. The thermal profile used to form the oleogels and acquire their clear and cloud points data was the one presented in Table 1.

Table 1
Thermal profiles used for the formation of the oleogels.

Step	Starting Temperature [°C]	Ending Temperature [°C]	Ramp [°C/min]	Holding Time [min]
1	20	80	10	10
2	80	60	-10	5
3	60	20	-0.5	60
4	20	80	0.3	10
5	80	70	-10	5
6	70	20	-2	60

Clear and cloud points were collected using the CrystalClear Software (Technobis, Netherlands). The clear point corresponds to the temperature during heating at which the solution becomes completely transparent, signalling total dissolution, whereas the cloud point represents the temperature during cooling at which turbidity first appears due to the onset of crystallisation (indicated by a drop in transmissivity). Oleogels referred to as "Static" were prepared for all concentrations of RBXP by applying a stirring rate of 780 rpm during steps 1, 2, 4 and 5, and stopping the stirring during cooling steps 3 and 6. On the other hand, oleogels referred to as "Stirred" were prepared only using 1%wt and 5%wt RBX concentrations by applying a constant stirring during all the steps of the oleogelation process. These two concentrations were chosen as 1%wt was determined as the lowest amount of RBXP necessary to form a stable oleogel, and 5%wt was the highest concentration which guaranteed the least noisy transmissivity in the Crystal 16 apparatus. The stirring rates tested were 300 rpm, 420 rpm, 540 rpm, 660 rpm, 780 rpm, and 900 rpm. These two different conditions were tested to assess how stirring conditions influence the oleogel formation. Once the oleogels were prepared, they were characterised to examine their thermal, structural, and rheological features.

2.4. Stability assessment and polarised light microscopy characterisation

After the process in the Crystal 16 equipment ended, the hook impellers were removed and the oleogels were left to settle for a week. To visualise the effect of applying stirring during the oleogel formation phase, pictures of the vials were taken using a Samsung Galaxy A51 (Samsung, South Korea). The microstructural differences for all the different oleogels prepared (replicates included) were analysed through Polarised Light Microscopy (PLM). A bead of oleogel was withdrawn from the vial with a spatula and carefully smeared in the central part of a glass slide, then covered with a cover glass. The glass slide was then positioned on a Zeiss Axiolab 5 microscope (Zeiss, Germany) with a polarised light lens. Pictures were taken using a 10X magnification lens using again a Samsung Galaxy A51. The post-processing of the images acquired was conducted using ImageJ 1.54d software (USA). The software was used to insert scale bars in order to provide orders of magnitude for the images acquired for qualitative purposes.

2.5. Thermal characterisation

Differential scanning calorimetry (DSC) was used to highlight the differences in the melting and crystallisation temperatures of the RBXs and their oleogels. A DSC200-Hitachi (Hitachi, Japan) was used to acquire the heat flow measurements. The preparation involved weighing and sealing each sample in an aluminium pan, with an empty pan serving as the reference. For RBX samples, a weight of around 4 mg of material was used; for RBX/SO oleogels the quantity used was between 6.5 mg and 8 mg. The RBX samples were heated from 0°C to 100°C with a ramp of 5 °C/min and then cooled again to 0°C with a ramp of −2 °C/min, for consistency with the measurements conducted in Candela et al., 2025. Since dissolving RBX in SO shifts the phase transition temperatures towards lower temperatures, the heating and cooling for the RBX/SO oleogels were both set between −40°C and 80°C with ramps of ±5 °C/min. Experiments were performed in duplicate under a 50 mL/min nitrogen purge.

2.6. Structural characterisations

2.6.1. Synchrotron SAXS/WAXS

Structural insights into RBX and RBX/SO oleogels were obtained through Small-Angle / Wide-Angle X-ray Scattering (SAXS/WAXS) measurements at the ID02 beamline of the European Synchrotron Radiation Facility (ESRF, France) and at the offline SAXS facility at Diamond Light Source (DLS, UK).

The experimental setup at ESRF featured a commercial ThermoHaake RS6000 rheometer (Thermo Fisher Scientific, Germany) coupled with a polycarbonate Couette geometry, allowing for simultaneous rheological and structural characterisation. The experimental configuration employed an Eiger2 4 M detector (Dectris, CH) for SAXS ($0.45 < q < 5.8\ nm^{-1}$) and a Rayonix LX 170HS (Rayonix, US) for WAXS ($5.68 < q < 35.17\ nm^{-1}$), both operating with a beam energy of 12.5 keV ($\lambda = 1$ Å). RBX/SO oleogels prepared with RBXP were melted and a quantity of around 2.5 mL was poured inside the Couette. Samples were brought to 80°C and left at this temperature for around 15 min. Then, temperature was cooled to 70°C with a ramp of −1 °C/min and kept for 5 min. A final ramp to 25°C of −1°C/min concluded the thermal profile. Measurements in shearing conditions were conducted with a constant shear rate ($\dot{\gamma}$) of 1000 1/s.

At the DLS labSAXS laboratory, SAXS and WAXS data were collected using an Eiger 2 R 1 M (SAXS) (75 micron) and a Pilatus 3 R 100 K (WAXS) (172 micron) detector (Dectris, CH), respectively, with an Excillium Ga MetalJet −9.2 keV as an electron source. Silver behenate (d-spacing 58.38 Å) and p-bromobenzoic acid served as calibration standards. Samples were loaded into quartz capillaries (1.4 ± 0.1 mm diameter) in their melted state using a 120 mm needle syringe. A Linkam capillary stage CI94 (Linkam Scientific Instrument, UK) was used to control the temperature ramps applied to the samples. The thermal protocol involved an initial cooling down to −5°C, followed by a heating step up to 90°C at 2 °C/min. Subsequently, the temperature was ramped down to 25°C at −10 °C/min. Data processing was performed using the Peak Analyzer tool in Origin 2018 (OriginLab Corporation, USA).

2.6.2. Rheological measurements

The sample with a 5%wt concentration of RBXP, RBXA, and RBXB in SO were subjected to further rheological assessments. Rheological properties were investigated with an Anton Paar MCR 302 (Anton Paar, Austria) rheometer using a parallel plate setup (25 mm diameter) at a constant gap of 0.5 mm. A bead of the sample to be analysed was spread on the rheometer plate at 25°C and, before starting the measurements, a time period of two minutes was allocated for the sample to reach equilibrium. For the rotational analysis, the shear rate was varied between 10^{-1} and 10^{2} 1/s. The amplitude sweep tests were conducted with a frequency of 5 Hz, while the frequency sweep tests were conducted with amplitudes of 0.05%.

2.7. Statistical analysis

Statistical analysis was performed using RStudio software. A one-way analysis of variance (ANOVA) was conducted to evaluate the effect of the experimental treatments (wax concentrations, extent of agitation, and type of wax) on the measured parameters (T_{clear} and T_{cloud} for the oleogels, melting and crystallisation enthalpies for the waxes). When overall statistical significance was established, Tukey's honestly significant difference post-hoc test was applied to perform pairwise comparisons between group means. Differences were considered statistically significant at $p < 0.05$.

3. Results and discussion

3.1. Chemical characterisation

3.1.1. LC analysis

The aliphatic components of the wax samples were determined by LC-ELSD with a method targeting wax esters, free fatty acids, fatty alcohols and n-alkanes. The chromatograms and the relative mass fractions of the wax ester fraction are shown in Fig. 1.

The chromatograms show that all three waxes are mainly composed of long-chain wax esters within a carbon number range from 42 to 60 in the retention time region between 26 and 37 min. At lower retention times, only negligible peaks below the limit of quantification have been found. This composition is typical for RBX, which is typically reported to

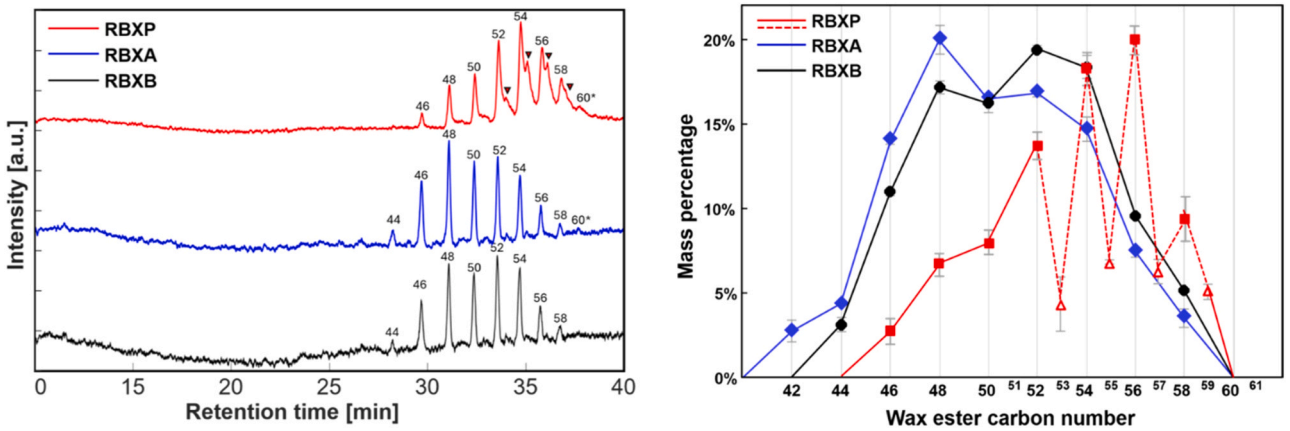


Fig. 1. LC-ELSD chromatograms and relative mass fractions of the wax ester fraction of the laboratory-extracted and commercial RBXs. Error bars represent the standard deviation of n = 3 measurements. *Peak below the limit of quantification.

contain 95–97%wt of wax esters (Doan, To, et al., 2017; Vali et al., 2005).

The major difference arising from the wax ester carbon number profiles is the quantitative wax ester distribution. While RBXA (blue) and RBXB (black) exhibit a fairly similar profile with wax esters of carbon number 48 being dominant, the overall carbon number distribution of RBXP (red) is shifted towards higher total carbon numbers. Here, wax esters with a carbon number of 54 are the dominant wax esters. Further, it is clearly visible that RBXP contains significantly higher amounts of odd wax esters than the commercial samples. The overall distribution is narrower for RBXP than for the commercial samples. The notable abundance of odd-carbon-number wax esters in RBXP likely reflects variations in the underlying plant tissue types or raw material origin compared to the commercial waxes, as biosynthetic pathways in specific rice bran fractions can yield varying fatty acid and alcohol precursor profiles. This may further influence the chain-length symmetry and overall crystal packing behaviour.

Even though the method focuses on the major aliphatic wax constituents, the data allow further conclusions on the composition. During the flushing step of the LC runs, the remaining sample which cannot be resolved by the column is washed off. For the commercial samples, a higher intensity at equal concentration was recorded, indicating a higher fraction of non-aliphatic components (see Figure S1).

In the results of the previous contribution (Candela et al., 2025), TAGs were suggested as one possible contaminant of RBX samples of lower purity. Dominant TAGs in RBO are composed of palmitic, oleic and linoleic acids (Miyazawa et al., 1978). Using the same analytical method, these would elute between 15 and 22 min with higher response factors that the other aliphatic components of waxes (data not shown). Therefore, the LC results discourage this hypothesis as this retention time window clearly shows no peaks for any of the waxes. Thus, while TAGs can be ruled out as primary contaminants, the chromatograms suggest that non-aliphatic or polar minor components are eluted during the flushing step.

3.1.2. FTIR analysis

The different RBX samples with different chemical composition were analysed regarding their functional groups using FTIR spectroscopy. The FTIR spectra of RBXP (red), RBXA (blue) and RBXB (black) are depicted in Fig. 2. Besides the dominant bands at 2916–2800 cm^{-1}, which are typical for the CH_2-backbone of hydrocarbon chains (Socrates, 2010), all three spectra show characteristic bands for the major components of natural waxes with low variation. At high wave numbers between 3550 and 3100 cm^{-1}, exclusively RBXA shows a broad band of low intensity. This is indicative of the presence of –OH stretching vibrations of hydroxyl groups and therefore attributed to free fatty alcohols. All three

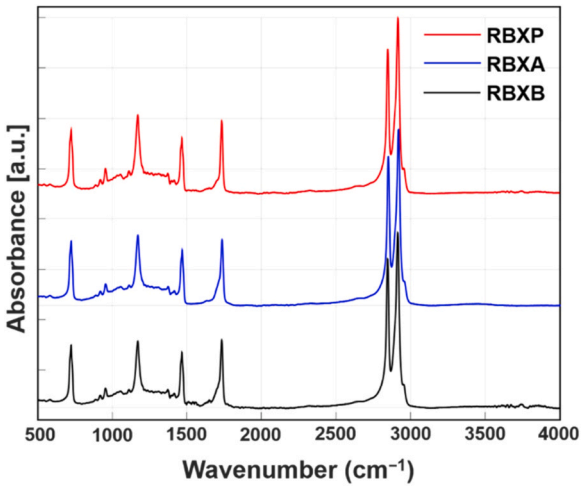


Fig. 2. FTIR spectra collected for the laboratory-extracted and commercial RBXs samples.

samples show a clear band at 1734 cm^{-1}, with the two commercial samples RBXA and RBXB exhibiting a more pronounced shoulder at 1704 cm^{-1}. These bands are caused by the C=O stretching vibrations, which are found in ester bonds (1734 cm^{-1}) and carboxyl groups (1704 cm^{-1}) (Socrates, 2010). This result is consistent with the wax-ester-dominated composition of the three waxes as shown by LC analysis and as described in the literature(Doan, To, et al., 2017; Vali et al., 2005). Further, for the commercial samples, smaller fractions of fatty alcohols (RBXA) and fatty acids (RBXB) are indicated. As the LC results did not indicate significant amounts of either component class, this indicates CN below the detection limit of the LC method (see (Brykczynski et al., 2026)). For further evidence, comprehensive GC analysis would be required.

No further differences between the three samples were observed, again reflecting the dominance of the wax ester matrix. Consequently, FTIR also provides information on the major chemical constituents of the waxes, while minor components such as phytosterols or γ-oryzanol (Champagne Elaine (2004); Gopala Krishna et al., 2006; MIYAZAWA et al., 1978) cannot be resolved reliably due to overlapping absorption bands and their low abundance.

3.2. Oleogelation of SO with RBX

SO was used as the oil phase of the oleogels, while RBXP was used as the oleogelator. RBXP was used at various concentrations in the

manufacture of oleogels to assess its suitability as a high added-value ingredient. Due to their long-chain ester composition, waxes efficiently structure vegetable oils through high hydrophobicity and low critical gelling concentrations (Blake et al., 2014; Dimakopoulou-Papazoglou et al., 2025). Moreover, being discarded during oil dewaxing, they represent a low-cost alternative to other oleogelators (Doan et al., 2018).

3.2.1. Static oleogelation

"Static Oleogelation" tests are those not involving agitation during the cooling phase of the oleogelation process. As described in **Section 2.3**, concentrations of 0.5%wt, 1%wt, 2%wt, 3%wt, 5%wt and 10%wt RBXP were used. The minimum oleogelation concentration was considered to be the lowest RBXP quantity at which the oleogel remained firm after its vial had been overturned or shaken. This was found to be 1%wt, as also reported in other works (Blake et al., 2014; Dassanayake et al., 2009; Samuditha et al., 2012; Toro-Vazquez et al., 2007). The PLM images shown in Fig. 3 supports this assumption.

As can be clearly seen, there is a considerable difference between the gel structure obtained at 0.5%wt and 1%wt. Obviously, this is due to the higher wax content of the 1%wt oleogel compared to the 0.5%wt counterpart. The concentration of RBX also affects the clear temperature (T_{clear}) and cloud temperature (hereafter referred to as oleogelation temperature T_{cloud}) recorded. These temperatures are summarised in Table 2. It is evident that with an increase in RBXP concentration in the formulations, there is a corresponding increase in the relative T_{clear} and T_{cloud}. The one-way ANOVA statistical analysis revealed a significant dependence of the measured temperatures on the concentration of wax used ($p < 0.05$). Interestingly, however, Tukey's post-hoc test showed a lower level of significance between the 3 and 5%wt samples ($p > 0.05$). As it can be seen from Table 2, this behaviour can be explained by the fact that there is very little difference between the respective temperature values recorded. Macroscopically, no visible phase separation was observed in oleogels one week after their preparation (Figure S2 of the Supporting Information); this indicates a good stability at room temperature within the time window considered.

Table 2
Clear and cloud temperatures recorded for RBXP/SO oleogels at different RBXP concentrations during static oleogelation process. Values are expressed as mean ± standard deviation.

Concentration [%wt]	Clear Temperature [°C]	Cloud Temperature [°C]
0.5	48.5 ± 2.12	43.5 ± 0.71
1	54.5 ± 0.71	49.7 ± 0.07
2	60.1 ± 0.14	55.5 ± 0.07
3	64.2 ± 0.21	59.0 ± 0.28
5	66.1 ± 0.35	60.0 ± 0.01
10	69.5 ± 0.35	64.8 ± 0.35

3.2.2. Stirred oleogelation

"Stirred Oleogelation" tests are those involving agitation during the entire oleogelation process. The behaviour of oleogels obtained with agitation was investigated only for samples with concentrations of 1%wt and 5%wt of RBXP in SO. Based on the static experiments, these two concentrations were determined to be the most appropriate as 1%wt was found to be the minimum concentration to obtain a stable oleogel, while 5%wt was determined as the highest tested concentration with a low noise level in the transmissivity data acquisition in the Crystal 16 apparatus. The application of stirring appears to affect the network formation of the gels during cooling. As illustrated in Fig. 4, the compact gel structure that was obtained through the static process (Fig. 3) is now fragmented and divided into regions of smaller gelled agglomerates. This phenomenon also affects the stability of the oleogels, which begin to exhibit oil separation within few days of their preparation (as can be seen in Figure S2 of the Supporting Information).

Furthermore, it is possible to observe how the increase in agitation speed results in the formation of smaller agglomerates. This is evident when the oleogelation was conducted at 900 rpm with a concentration of 1%wt. It should be noted that these rotational speeds are strictly dependent on the vial and impeller geometry used in the Crystal 16

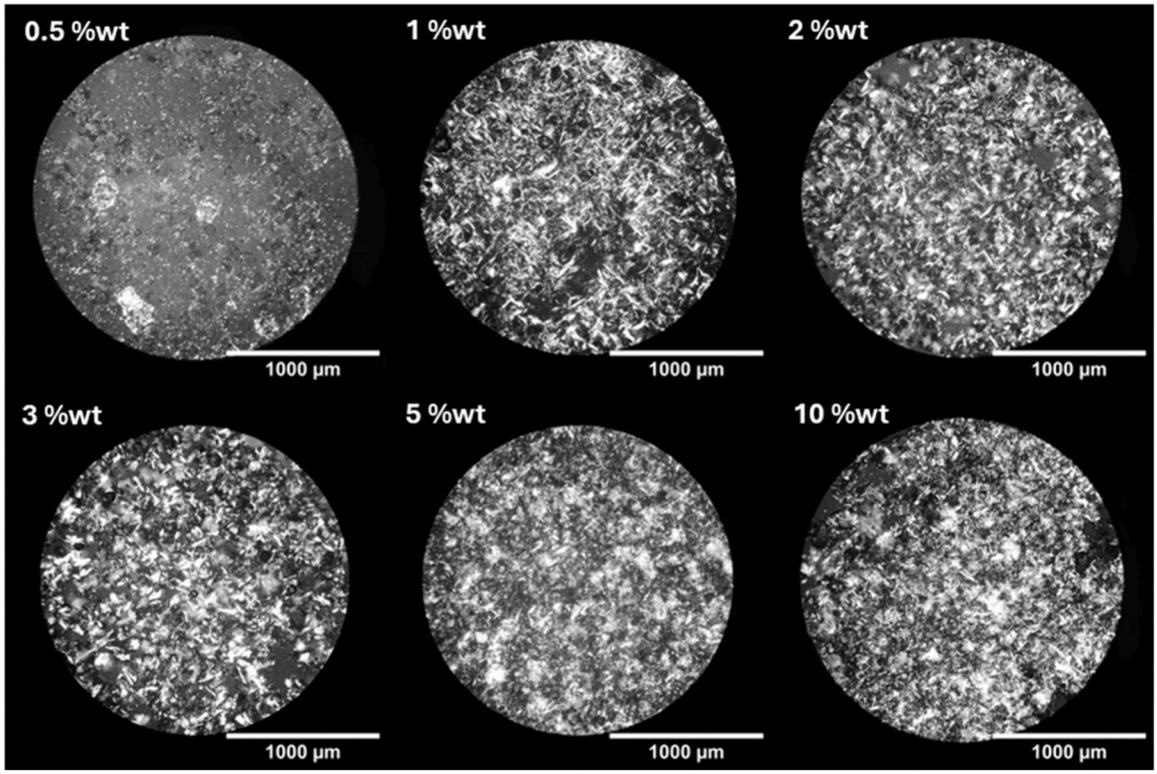


Fig. 3. PLM images of the RBXP/SO oleogels at Different Concentration formed with static cooling conditions, 10x magnification.

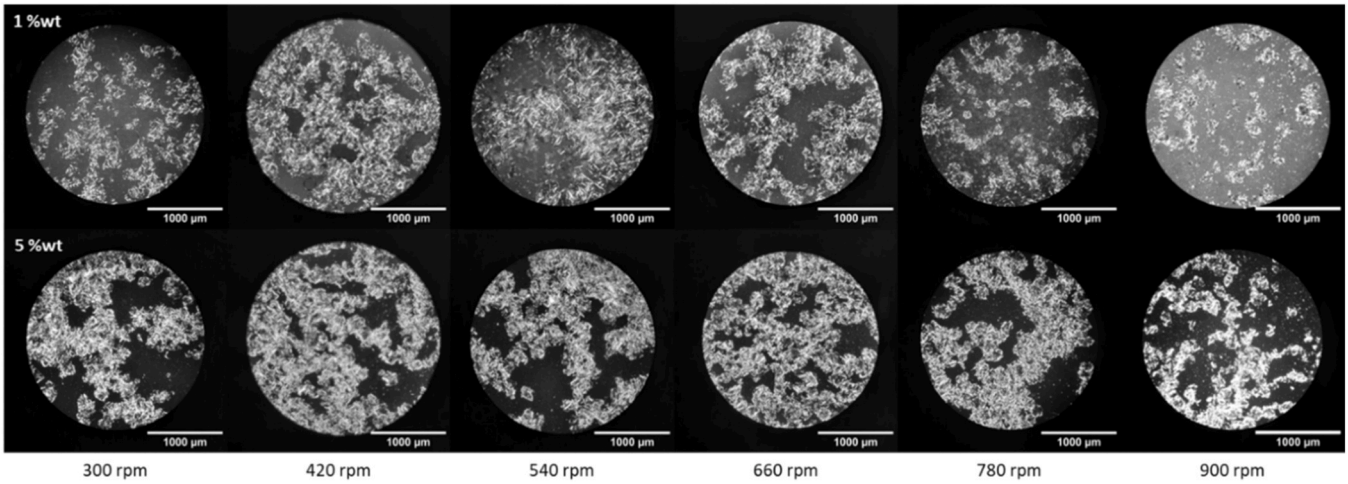


Fig. 4. PLM images of the 1%wt and 5%wt RBXP/SO oleogels at different stirring rates applied, 10x magnification.

apparatus, serving as relative indicators of mixing intensity for this specific setup. Subsequently, the recording of the T_{clear} and the T_{cloud} was conducted. The results are summarised in Table 3 and Table 4. While the clear point temperatures and the 5% wt cloud point temperatures showed no significant variation across the applied agitation rates ($p > 0.05$), the 1% wt cloud point temperature was significantly affected ($p < 0.05$). Specifically, Tukey's post-hoc analysis indicated that this difference stemmed primarily from the contrast between the static (0 rpm) and stirred conditions, pointing to a potential stirring-induced enhancement of aggregation during the cooling phase. In general, maintaining mechanical agitation for the entire duration of the cooling phase hindered the development of a continuous and fully interconnected three-dimensional oleogel matrix. In fact, the effect of shear hinders the formation of aggregates during cooling and the sintering of wax crystals to form a compact crystalline network. Since the mixing action was sustained throughout the whole slow cooling crystallisation step, non-connected solid crystals and small clusters formed and sedimented once stirring was stopped. Consequently, the observed macroscopic instability is specifically linked to this prolonged mechanical treatment. Different processing strategies (such as applying an initial mixing stage followed by quiescent cooling, or interrupting the agitation before the interconnected aggregates are formed) could potentially preserve the structural integrity of the network. The influence of these structural modifications on the network connectivity will be further detailed in Section 3.4.1.

3.2.3. *Performance evaluation against commercial alternatives*

To understand whether the separation during stirring was related to the chemical nature of RBXP, other oleogelation tests were conducted using RBXA and RBXB commercial waxes as oleogelators in SO. Again, 1%wt and 5%wt concentrations were taken as reference. At a concentration of 1%wt, for the oleogels with both commercial waxes in static and stirring conditions, the resulting networks appeared not to be completely formed. Compared to RBXP oleogels, these different formulations showed separation even in static conditions (Fig. 5). Using a 5%wt wax content in the same conditions of both RBXA and RBXB, on the other hand, seemed to produce a much more developed microstructure. Under stirring conditions, RBXB formed an oleogel that exhibited a lower extent of oil separation compared to both RBXA and the laboratory-extracted RBXP. This observation suggests that the minor components present in this specific commercial wax do not merely act as passive "impurities", but may functionally mediate inter-crystalline interactions. While the tight compositional homogeneity of RBXP leads to extensive flow-induced agglomeration under mechanical stress, the higher chemical heterogeneity in RBXB appear to mitigate this agglomeration, partially stabilising the three-dimensional network. In this perspective, although a highly uniform compositional profile favours an optimal structural connectivity in static environments, the presence of specific minor components can provide necessary resilience during dynamic processing.

Table 3
Clear and cloud temperatures recorded for 1%wt RBXP/SO oleogels at different stirring rates applied during oleogelation. Values are expressed as mean ± standard deviation.

Stirring Rate [rpm]	Clear Temperature [°C]	Cloud Temperature [°C]
0	54.5 ± 0.71	49.7 ± 0.07
300	55.2 ± 0.50	51.8 ± 0.57
420	55.7 ± 0.35	52.2 ± 0.07
540	56.4 ± 0.71	53.6 ± 0.35
660	56.1 ± 0.78	53.6 ± 0.07
780	53.1 ± 1.14	52.2 ± 0.61
900	54.0 ± 2.97	52.3 ± 1.84

Table 4
Clear and cloud temperatures recorded for 5%wt RBXP/SO oleogels at different stirring rates applied during oleogelation. Values are expressed as mean ± standard deviation.

Stirring Rate [rpm]	Clear Temperature [°C]	Cloud Temperature [°C]
0	66.1 ± 0.35	60.0 ± 0.01
300	65.0 ± 0.14	61.5 ± 0.28
420	64.8 ± 0.14	61.6 ± 0.21
540	65.7 ± 0.99	62.3 ± 1.20
660	65.5 ± 1.06	62.5 ± 1.20
780	64.7 ± 0.14	60.8 ± 1.11
900	64.7 ± 0.85	61.4 ± 1.13

3.3. *Thermal behaviour*

To better understand the thermal properties of the oleogels formed with RBXP, RBXA and RBXB, both the RBXs and the RBX/SO oleogels were analysed through DSC. Melting and crystallisation behaviour were recorded more precisely, and a finer comparison was conducted.

3.3.1. *Starting materials thermal behaviours*

Fig. 6 presents the thermogram related to RBXP, RBXA, and RBXB. Furthermore, as a comparison with that previously reported by Candela et al., 2025, another wax (RBX #5) is shown. This choice was made to compare how the different extraction history of the waxes (see comparison for chemical characterisation in Figure S3 of the Supporting Information) can influence the thermal features recorded during the

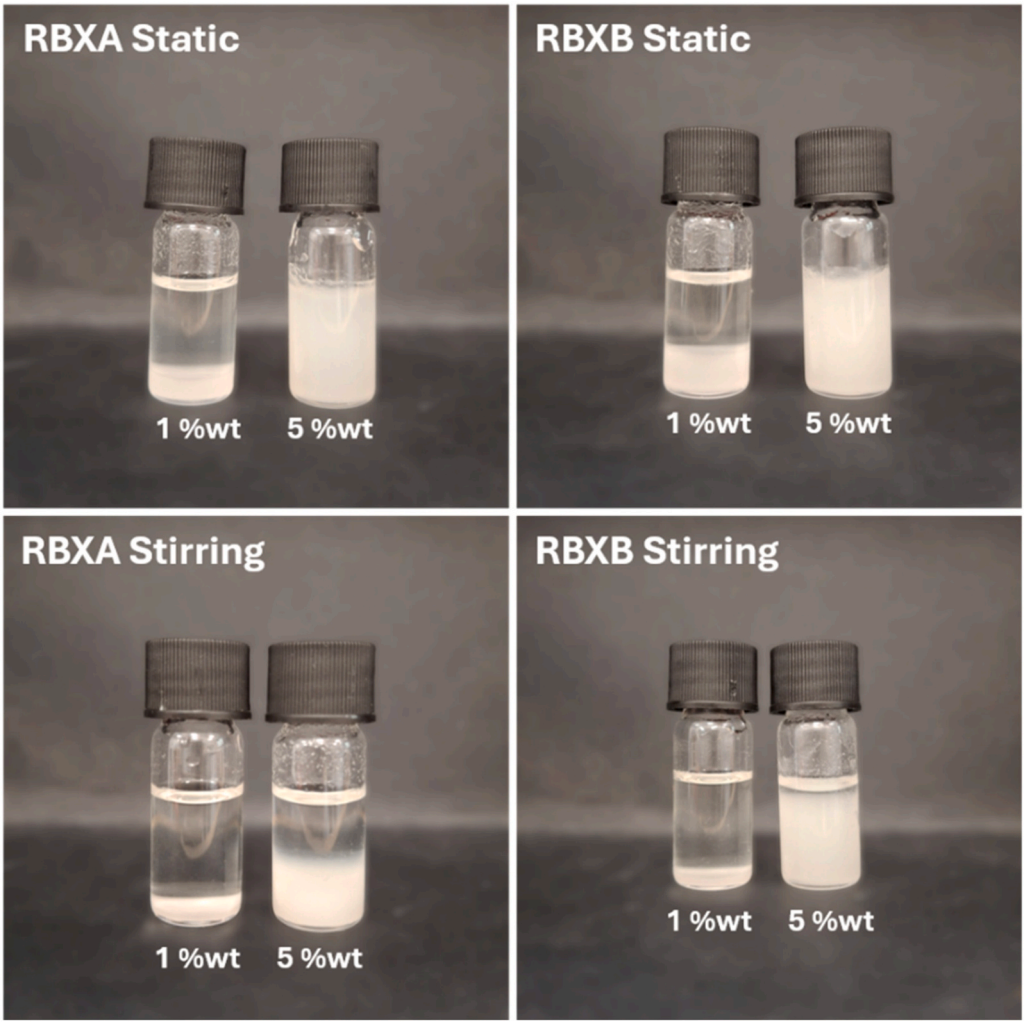


Fig. 5. Comparison between oleogels obtained with and without stirring in the oleogel formation step using RBXA and RBXB.

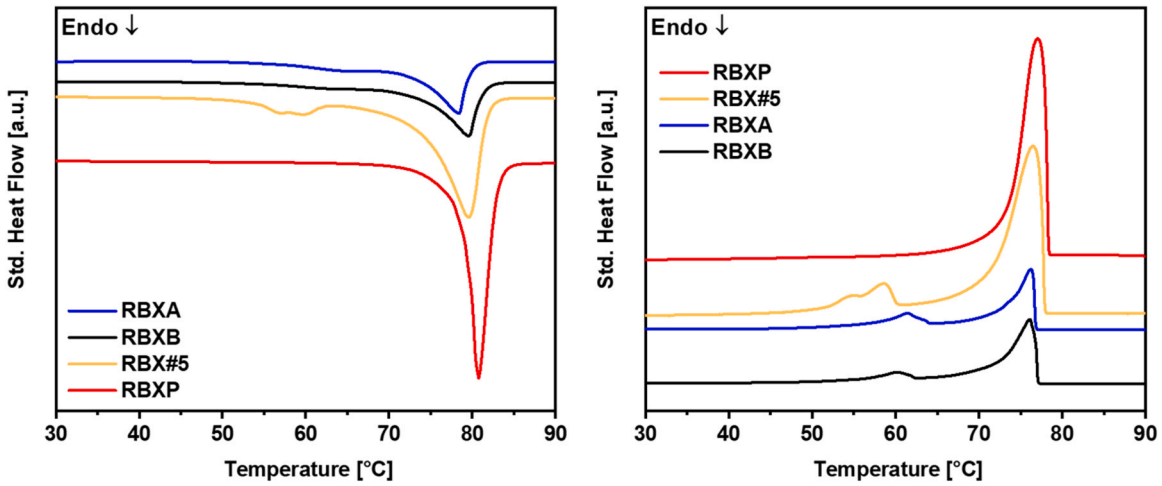


Fig. 6. Melting and crystallisation profiles of RBXs tested as oleogelators.

thermal analysis.

Firstly, one should consider the differences between RBXP (red) and RBX #5 (yellow). As already described in the relative paper (Candela et al., 2025), varying the purification method may lead to a different chemical composition in the final extract. In this previous study without comprehensive LC analysis, these compositional differences could not be resolved. The results obtained in the present study allow to assume either the presence of short-chain fatty acids and fatty alcohols below the detection limit of the ELSD or non-aliphatic minor components in the RBX which could affect the mixing phase and therefore thermal

behaviour of the different RBX samples. In the thermogram related to RBX #5 (yellow), two clear peaks between 50°C and 60°C are evident and might be related either these sorts of minor components or to the absolute presence of wax esters of the extract (above 70°C). Comparing the RBXs obtained by purification with the commercial RBXs, similar considerations can be formulated. Looking at the melting and crystallisation profiles, commercial waxes have broader peaks and different melting and crystallisation enthalpies, as shown in Table 5. A statistically significant difference was observed for the melting enthalpy among the samples ($p < 0.05$, one-way ANOVA). This is mainly attributed to the lower value recorded for sample RBX5 compared to the other RBXs. Post-hoc Tukey test, in fact, revealed a statistically significant difference between RBX5 and the other samples ($p < 0.05$), while it showed no statistical relevance among the other wax samples ($p > 0.05$). Conversely, no statistically significant differences were detected for the crystallisation enthalpy ($p > 0.05$), indicating a consistent thermal behaviour during the cooling phase across all samples tested. Comparing the extracted RBX with commercial variants, these thermal transitions reflect not only the presence of minor polar components but also a fundamental shift in the wax-ester profile itself. In the temperature interval below 70°C, both RBXA (blue line) and RBXB (black line) showed a broad and low-intensity peak, a feature becoming more visible when looking at the crystallisation profiles. Commercial waxes exhibit a broader chemical distribution dominated by wax esters with CN48, whereas RBXP is dominated by CN54 esters with a narrower distribution and a notable proportion of odd-carbon-number esters. A broader carbon-number spread typically promotes fractionated crystallisation or phase separation, which corresponds to the broad, low-intensity transitions observed below 70°C for RBXA and RBXB (Fig. 2). Conversely, the higher average chain length and sharper chemical distribution in RBXP might cause more uniform crystal packing, higher crystallisation temperatures, and stronger static gelation networks. These characteristics are reflected in the relative melting and crystallisation enthalpies, which resulted higher for commercial waxes compared to the purified ones. On the other hand, this different composition extent seems also to have a disadvantageous effect when applying stirring during the oleogelation step. The greater affinity that the wax-esters molecules have among each other might led to the gelled aggregates formation. These aggregates tend to settle at the bottom of the vials leading to the instability of the corresponding oleogels and to oil leakage.

3.3.2. 5%wt oleogels thermal behaviours

In this subsection, the thermal behaviour of the oleogels formed with RBXP, RBXA, and RBXB in SO is presented. Only data related to the 5% wt concentration of RBXs are shown since the peaks recorded are more visible with this RBX content. Fig. 7 shows the results related to the DSC analysis performed on these oleogels.

As it can be expected, the melting and crystallisation profiles of the oleogels formed with RBXP (red) show less defined and narrower peaks compared to the starting wax. Compared to the other oleogels formed with commercial waxes, the RBXP/SO oleogel manifests a sharper and more uniform melting transition. In RBXP/SO oleogel, only a single melting and crystallisation event is recorded. For oleogels prepared with the commercial waxes, by contrast, one can recognise multiple and broader peaks. This can be either related to minor components and their effects on network formation or to the different wax ester carbon number profiles (see Fig. 1). Although the complex mixing phase behaviour of individual wax esters remains to be comprehensively resolved, these compositional differences certainly play a decisive role in network formation and stability. Under stirred oleogelation conditions, however, this high self-affinity of long-chain esters in RBXP may promote localised aggregation rather than an extended continuous network, ultimately predisposing the gel to phase separation and oil leakage.

Comparing with the starting RBXP thermal profiles, the oleogel's melting and crystallisation peaks are moved towards lower temperatures due to dissolution of the wax in SO, which is liquid at ambient temperature (Blake et al., 2014; Holey et al., 2021; Wijarnprecha et al., 2018).

Table 5
Melting and crystallisation mean value enthalpies with standard deviation comparison of the purified and commercial RBXs.

RBX type	Melting Enthalpy [J/g]	Crystallisation Enthalpy [J/g]
RBXP	190.08 ± 8.90	-179.77 ± 10.75
RBX#5	163.44 ± 1.84	-169.33 ± 9.04
RBXA	190.25 ± 4.03	-190.31 ± 9.19
RBXB	200.99 ± 4.09	-195.97 ± 0.66

3.4. Structural features

3.4.1. Rheo-SAXS comparison of RBXP/SO oleogels

The 1%wt and 5%wt samples were analysed using synchrotron SAXS/WAXS. Tests were conducted at both static and constant shear rate ($\gamma = 1000\ s^{-1}$) conditions provided by the rheometer (see **Section 2.6.1** for further details). Fig. 8 shows the relative diffractograms collected with samples of 5%wt RBXP in SO.

A comparison between the graphs of the oleogels with those of the pure wax (Candela et al., 2025) clearly demonstrates that the blending process with SO has a notable impact on the recorded signal. In the oleogels, a single polymorph is evident in the SAXS region, appearing at around 80°C during cooling. The first peak of this polymorph appears at $q = 0.88\ nm^{-1}$ (D-spacing = 7.14 nm) and can be attributed, considering also the WAXS region, to an orthorhombic perpendicular subcell frequently recorded with waxes obtained from plant-based matrices (Pandolsook & Kupongsak, 2020). Furthermore, by looking at the second and third order reflections a broadening of the peaks can be observed, suggesting a possible presence of a segregated crystallisation and overlapping of multiple phases. In the pure RBXP diffractograms, other polymorphs are also observed; however, the blending with SO reduces their signal's intensity and these are not recorded in the oleogel samples. In the WAXS region, the peaks collected are also related to the presence of the orthorhombic perpendicular subcell. A comparison between the oleogel samples obtained with a constant shear rate (applied by the rheometer) and without shear revealed no substantial differences in terms of polymorphism. This observation is not in contrast with the macroscopic behaviour detailed in Section 3.2.2, where impeller-driven flow was shown to severely compromise the physical stability of the oleogels. Indeed, the applied fluid dynamic forces primarily affect the wax crystal aggregation and the formation of an efficient spatial connectivity within the network, without altering the local nano and sub-nanoscale of wax-ester crystal structure. While shear is known to influence polymorphic crystallisation in other lipid systems like cocoa butter [51], [52], the primary crystal form of the RBXP/SO oleogels does not seem to be affected by shear. Furthermore, it must be noted that the appearance of the first crystalline phase in the SAXS region occurs at approximately 70–80 °C (for 1%wt and 5%wt, respectively). These temperatures are substantially higher than the T_{cloud} (roughly 50 - furthermore 60 °C) recorded with the Crystal 16 apparatus. This discrepancy can be attributed to the different length scales probed, the detection sensitivities, and the distinct thermal and fluid dynamic histories of the two experimental setups. SAXS is highly sensitive to the initial formation of nanoscale crystalline domains, thus detecting the primary nucleation events of wax crystals as soon as they form. Conversely, the Crystal 16 relies on macroscopic light transmission, meaning a cloud point is registered only when crystals have grown and aggregated into structures large enough to scatter visible light. Additionally, the differences in experimental geometries (e.g., Couette cell in the rheometer vs. impeller-agitated vial) and cooling rates (-1 °C/min for SAXS vs. −0.5 °C/min for Crystal 16) create different mixing regimes that inevitably delay or accelerate the onset of macroscopic turbidity

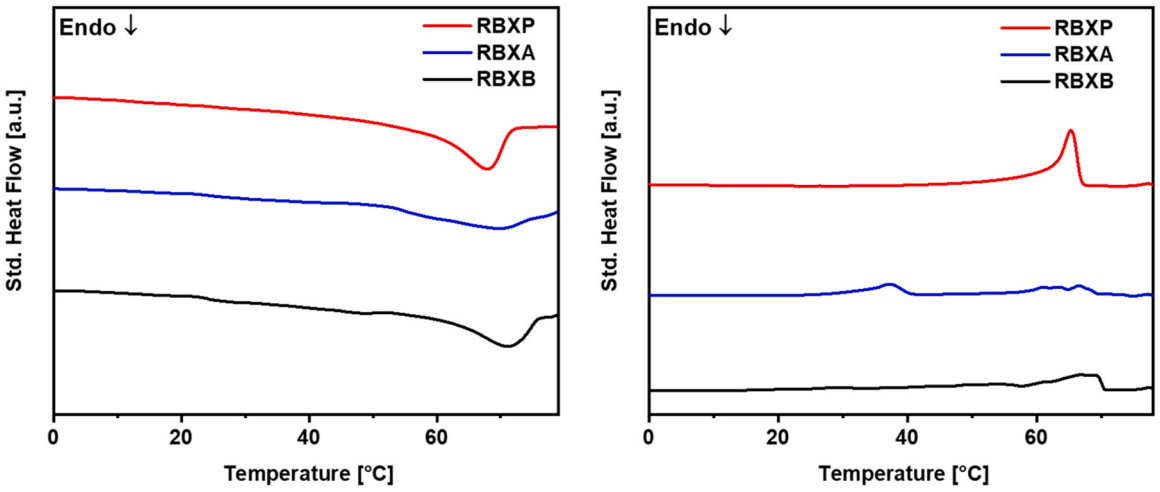


Fig. 7. Melting and crystallisation profiles of 5%wt RBXs/SO.

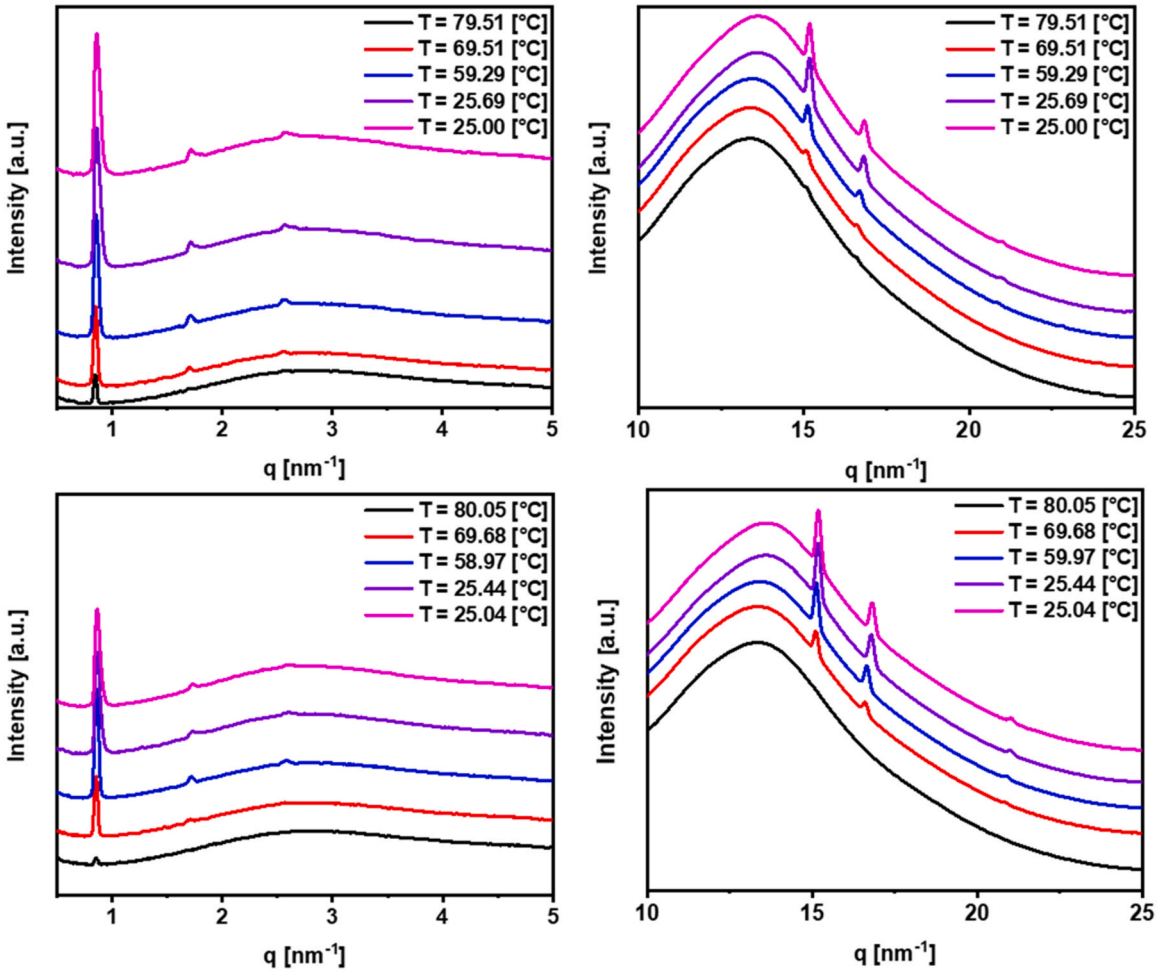


Fig. 8. SAXS (left side) and WAXS (right side) diffractograms of the 5%wt RBXP/SO oleogel. Comparison between data recorded without (top part) and with (bottom part) constant shear rate ($\gamma = 1000\ s^{-1}$) applied.

compared to the nanoscale nucleation phenomenon. Figure S4 shows the same results presented in Fig. 8 but obtained with the 1%wt RBXP/SO samples. The only differences between these two concentration samples rely on the temperatures at which the crystalline phase appears: in the 1%wt sample it appears at 70°C during cooling (around 10°C of difference compared to the 5%wt sample as also previously shown in the cloud temperatures and DSC data).

SAXS and WAXS profiles were also collected for pure RBXA and RBXB, and for their relative oleogels prepared at the concentration of 5% wt of wax in SO. Since these samples were not analysed at the same beamline and with a different setup, only capillary measurements could be collected. The relative data are presented in Figures S5 and S6. Both

the pure materials only showed a single polymorph with its first peak at around q = 0.87 nm^{-1} and a corresponding D-spacing of 7.22 nm. These values can be attributed to a similar crystallisation pattern as for RBXP (an orthorhombic perpendicular subcell). For both waxes the related peaks disappear around 82°C, as also presented in the thermal characterisation section. For the oleogels prepared starting with these two materials, the signal appears noisy (possibly due to the high quantity of oil inside the samples). In any case, one can distinguish again the same polymorph with the first peak in the very same position. In the oleogel RBXA/SO the only visible peak seems to melt at a slightly lower temperature compared to RBXB/SO. This behaviour is in agreement with the DSC measurements previously discussed.

Overall, comparing the systems obtained with the recovered refined wax and the commercial counterparts, no notable differences can be recorded or attributed to the nature of the waxes. These findings confirm that sample crystallisation is dominated by the RBXs wax esters, the most abundant components. From the chemical characterisation it was noted that these resulted there were not significantly different. This suggests that the microstructural and functional differences of the oleogels might be affected by the interactions upon network formation and crystals aggregation, and dominated by other components that was not possible to detect with the analysis performed. All these considerations highlight what can be a critical area for future analytical focus.

3.4.2. *Rheological characteristics of RBXP/SO oleogel*

A first rheological assessment of the oleogels was conducted by recording the viscosity evolution of the samples during the SAXS/WAXS measurements in the Rheo-SAXS environment at the ESRF ID02 beamline. As it can be noticed in Fig. 9, the increase in the RBXP concentration induces an increase in the apparent viscosity recorded during the cooling of the samples. This is an expected effect due to the difference in the wax content in the samples. In this regard, RBXP in higher concentrations immobilises more oil in the 3D structure of the oleogel, leading to an increased resistance to the shear rate applied (Wijarnprecha et al., 2018).

To better understand the mechanical features of the RBXP/SO oleogel systems, a complete rheological characterisation was conducted on the 5%wt sample. This sample was chosen as a benchmark because using a greater amount of wax than 1%wt resulted in a more accurate data from the instrument.

The amplitude sweep test was utilised to evaluate the oleogel's structural integrity and robustness prior to failure. The test is designed to identify the linear viscoelastic region (LVR), defined as the range of percentage strain within which the oleogel's behaviour can be considered viscoelastic (Doan et al., 2015). Fig. 10 shows the results obtained applying a frequency of 5 Hz. The gel-like behaviour is justified by the values of the storage modulus G' and the loss modulus G''. As a matter of fact, in the LVR, the elastic modulus (G' ≈ $2 \cdot 10^4$Pa) is markedly higher than the viscous modulus (G'' ≈ $7 \cdot 10^3$ Pa). The high absolute value of the modulus G' confirms the effectiveness of the RBXP in forming a robust crystalline network, capable of a distinctly solid and elastic behaviour at rest. However, the recorded LVR appears to be rather short: in fact, both curves begin to drop rapidly before 0.1% strain. This results in a crossover (G' = G'') and, consequently, gel rupture at approximately 0.6% strain. These observations highlight the brittle nature of the developed oleogel structure, which exhibits low elastic resistance before the structural breaking. Similar observations were done by Doan et al., 2015, who found that RBX is able to produce an oleogel with a limited extent of LVR compared to other waxes. The crucial factor highlighted in that work is the affinity between the wax and the oil used, which can determine the strength of the resulting oleogel (Doan et al., 2015).

The identification of the strain range where the oleogel presented a viscoelastic behaviour, allowed the determination of the strain value for the frequency sweep tests (Fig. 10). This was 0.05% before the rapid drop of the moduli in the amplitude sweep test identified inside the LVR. By varying the frequency in the explored interval, the elastic modulus always showed higher values compared to the loss modulus. The same trend was recorded in other works using RBX as an oleogelator, where G' was never found to have a crossover point with G'' during frequency sweep tests (Doan et al., 2015; Principato et al., 2021; Wijarnprecha et al., 2018). This profile is indicative of a structured system

exhibiting a solid-like behaviour, suggesting that RBXP forms a crystalline framework that can remain stable over time. The solid and elastic behaviours of the oleogels are also justified by the damping factor (tan (δ) = (G''/G')) profiles by varying the frequency applied (Fig. 11). At all the points of the explored frequency range, in fact, the value of the damping factor stays below 1, indicating the prevalence of the elastic properties compared to the viscous properties.

Finally, the flow behaviour of the oleogel was evaluated considering complex viscosity and viscosity curves. Measurements were repeated in triplicate and are presented as the first, second, and third trials in Figs. 11 and 12.

As shown in Fig. 12 (left side), the sample exhibited a marked non-Newtonian behaviour, with the steady-state viscosity (η) decreasing by several orders of magnitude as the shear rate increased (Principato et al., 2021; Wijarnprecha et al., 2018). However, some fluctuations can be observed in the recorded shear stress profile (Fig. 12, right side): these indicate the presence of non-uniform fracture of the oleogel or wall slippage during the measurement, confirming the high mechanical fragility of the gel 3D-network previously detected during the amplitude sweep test. To mitigate wall slip and confirm these observations, alternative setups (such as slip-resistant geometries or roughened plates) should be considered for future assessments.

The commercial waxes RBXA and RBXB were also used to prepare two oleogels (5%wt of RBX each) for comparison with the RBXP. Comparing the relative amplitude sweep tests performed at 5 Hz (Figure S7), a rapid decrease of both G' and G'' is visible for both samples. For RBXA the crossover point seemed not to be completely reached: this is a common behaviour of highly viscous fluids. RBXB, instead, exhibited a crossover point at around 2% strain (higher than the 0.6% strain recorded for RBXP-based oleogels). For both RBXA and RBXB oleogels, the loss and storage moduli had comparable values with similar order of magnitude. In contrast, RBXP oleogel presented values greater than two orders of magnitude, suggesting the presence of a more robust and cohesive structure compared to the commercial waxes.

Looking at the results obtained with the frequency sweep tests at 0.05% of fixed strain (Figure S7), again the differences in G' and G'' values are evident: as expected, considering the results of the amplitude sweep test, the RBXP oleogel had higher values compared to the RBXA

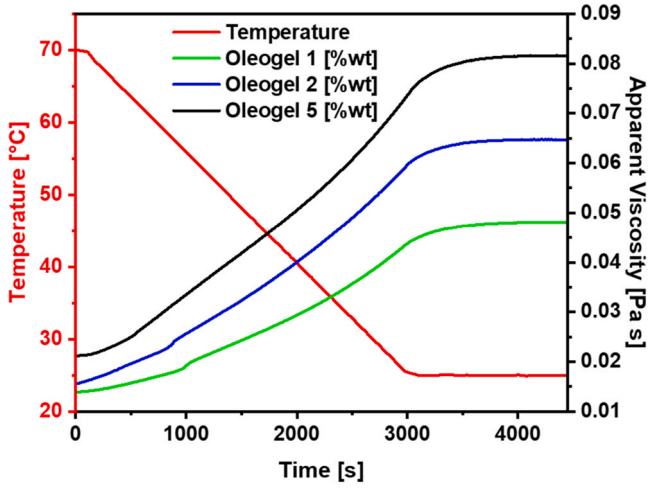


Fig. 9. Changing of the apparent viscosity of RBXP/SO oleogels during crystallisation. Measurements conducted at constant shear rate ($\gamma = 1000\ s^{-1}$) in the Rheo-SAXS environment of ID02 beamline of ESRF, Grenoble.

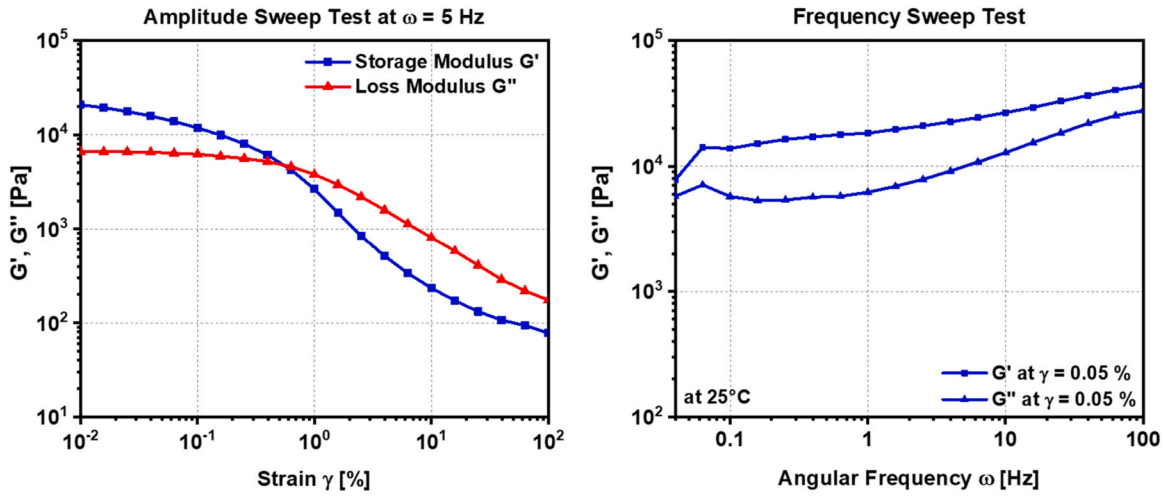


Fig. 10. Amplitude Sweep test results investigated at 5 Hz fixed frequency (left side); Frequency Sweep test results investigated at 0.05% of fixed strain (right side).

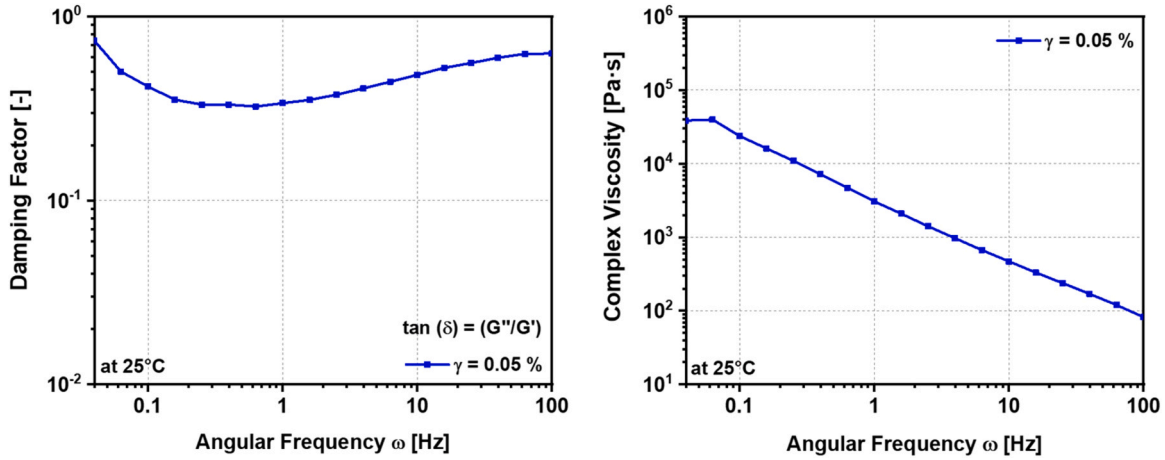


Fig. 11. Damping Factor (left side) and Complex Viscosity (right side) recorded during the Frequency Sweep oscillatory analysis at 0.05% of fixed strain.

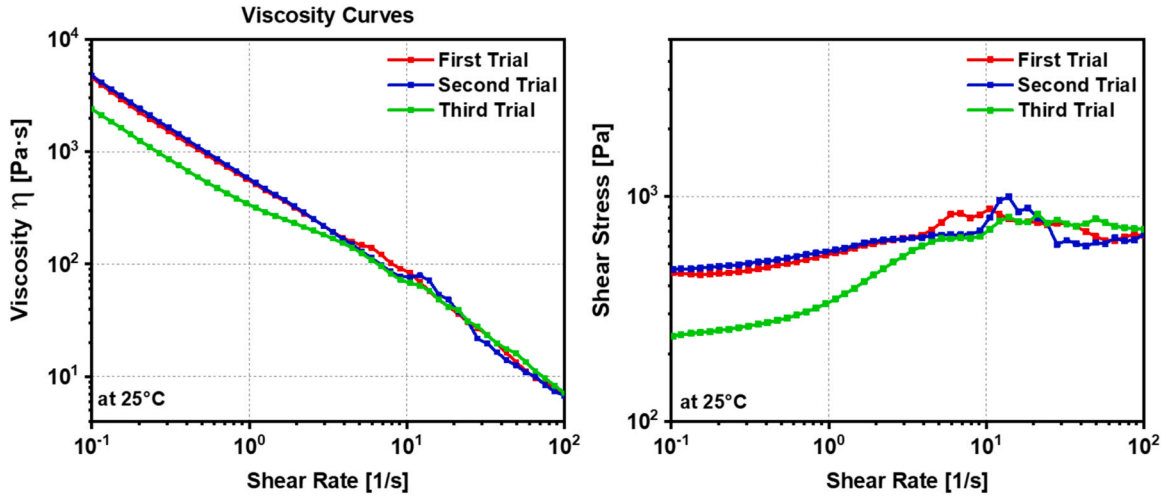


Fig. 12. Viscosity Curves (left side) and Shear Stress Profiles (right side) recorded during the rotational analysis.

and RBXB oleogels. In the RBXB-based oleogel profiles, G' and G'' never presented a crossover point (similar behaviour of RBXP-based oleogel), while for the RBXA-based sample multiple crossover points are present after the frequency of 6 Hz is reached. This behaviour suggests a strong instability of the RBXA-based sample that compromised the data acquisition compared to the other two oleogels. This consideration could also be supported by the evolution of the damping factor (Figure S8): RBXA-based sample is the only oleogel which presented values

approaching 1 and becoming higher after the frequency of around 6 Hz is reached. In this perspective, we could affirm that RBXA was not able to produce a stable oleogel in all the range of shear investigated. Looking at the complex viscosity recorded for both the oleogels prepared with the commercial waxes, the sample prepared with RBXB exhibits a systematically higher complex viscosity values than the one prepared with RBXA across the entire frequency range, indicating a denser and more compact internal structure. At angular frequencies above 10 Hz, both samples exhibit an upward trend in complex viscosity, which could stem from high-speed instrumental artefacts rather than the examined material behaviour. Finally, the more cohesive and resistant structure of the RBXB-based oleogel compared to RBXA-based one, is appreciable by looking at the Viscosity vs Shear Rate graphs (Figure S9). The values recorded are higher than those of the RBXA-based oleogel, but notably lower than those of the RBXP-based sample. Considering the comparison of all the rheological data acquired for all the wax samples, the laboratory-extracted wax seemed to produce a stronger oleogel which exhibits a high stability for all the ranges of the assessments performed. It is highly probable that the specific chemical composition of the RBX used led to a different degree of stability of the oleogels produced. When tailoring RBX-based oleogels for specific applications, it is therefore essential to consider how variations in the chemical species distribution within RBX's profile affect the firmness and flow properties of the resulting oleogel. It is important to stress some of the limitations of this set of rheology experiments. The tests carried out on the oleogel prepared with RBXP were conducted in three independent replicates only for the viscosity measurements due to limited availability of the RBXP samples. Similarly, or the amplitude sweep test and the frequency sweep test, it was not possible to carry out replicates. Additionally, it is worth reminding that the waxes tested were not isolated from exactly the same substrate; hence, differences in extraction but also in the initial composition are responsible for the different rheological behaviours.

4. Conclusions

The growing demand for sustainable and healthy ingredients has pushed research toward innovative systems that can provide nutritional benefits without compromising texture and sensory profile. Oleogels are of particular interest due to their ability to create a three-dimensional network by using an oleogelator to structure liquid oils. Among the various structuring agents, RBX has emerged as a promising candidate. However, the functional success of RBX-based oleogels is heavily dependent on the specific compositional profile of the wax, due to residual minor components that can interfere with the formation of the lipid network. Three different RBXs have been used in this study. The specific compositions were analysed using LC-ELSD and FTIR, demonstrating their different compositions. While all three waxes were mainly composed of long-chain wax esters, the carbon number profile between the commercial samples and the laboratory recovered RBX differed substantially with the commercial waxes, showing broader distributions lacking in odd wax esters. Minor fractions of free fatty acids and alcohols have been indicated. These compositional differences propagated into the functional properties. The specific composition of the RBX obtained through Process #2, with its lipid profile and narrow melting range, directly influences the microstructural development of the oleogels prepared. In particular, within the concentration range investigated under static gelation conditions, this homogeneity could be responsible for optimal spatial interlocking of the crystals and the formation of a continuous lipid framework, resulting in enhanced stable oleogels compared to the commercial alternatives (RBXA and RBXB). Furthermore, it was observed that the use of stirring during the oleogelation phase hindered the development of a solid framework. The high affinity among the highly homogeneous RBXP molecules led to extensive agglomeration under flow, compromising oil entrapment and resulting in discrete oil leakage. Interestingly, commercial waxes like RBXB retained oil more effectively under stirring, suggesting that minor components are not necessarily detrimental; rather, they could possibly promote a stabilisation effect against mechanical stress. In conclusion, this research highlights that the development of high-performance oleogels is strictly dependent on the interplay between the wax compositional profile and the processing regime. The results demonstrate that optimised isolation protocols could transform rice industry by-products into high-value ingredients that can possibly replace existing commercial alternatives, ensuring uniform properties across products. However, as the analytical methods used to characterise the chemical composition in this publication target the major constituents, alternative methods focusing on the minor components might be relevant for further specification. These minor impurities (possibly resulting from sterols, oryzanols and/or glycolipids) seem to not affect the primary crystallisation process but may have a crucial functional role in modulating inter-crystalline interactions in the mesoscale. Furthermore, in the future it would also be necessary to carry out tests to ensure that no residual solvent from the extraction process is present in the final oleogels, to meet the required standards for hypothetical food applications. Moving forward, these findings pave the way for several strategic developments. The stability of the chemically uniform RBX network suggests that it would be worth investigating in future how these systems perform when incorporated into food matrices, such as bakery products or spreads. Ultimately, this work supports the transition towards a circular bioeconomy, offering a plausible, sustainable, clean-label alternative solution for the formulation of lipid-based food products.

CRediT authorship contribution statement

Danilo Candela: Writing – original draft, Investigation, Formal analysis, Data curation, Conceptualization. **Henriette Brykczynski:** Writing – review & editing, Methodology, Investigation. **Cecilia Fiore:** Writing – review & editing, Investigation. **Eckhard Flöter:** Resources, Methodology, Funding acquisition. **Elena Simone:** Writing – review & editing, Supervision, Methodology, Funding acquisition, Data curation, Conceptualization.

Declaration of Competing Interest

The authors declare that they have no known competing financial interests or personal relationships that could have appeared to influence the work reported in this paper.

Acknowledgements

This project has received funding from the European Research Council (ERC) under the European Union's Horizon 2020 research and innovation programme (grant agreement No. 949229, CryForm), and the European Union's Horizon Europe research and innovation programme (grant agreement No. 101189244, NewOilFactory). Additionally, it was carried out within the Agritech National Research Centre and received funding from the European Union Next-GenerationEU (PIANO NAZIONALE DI RIPRESA E RESILIENZA (PNRR) – MISSIONE 4 COMPONENTE 2, INVESTIMENTO 1.4 – D.D. 1032 17/06/2022, CN00000022). We acknowledge ESRF and Diamond Light Source (DLS) for beamtime on beamlines ID02, and LabSAXS under proposals SC-5464 (ESRF) and SM44335–1 (DLS). We are grateful to beamline scientists Dr Thomas Zinn (DLS), and Dr William Chevremont (ESRF) for the help and support with the two SAXS beamlines and setups used for the work. We would like to thank Mr Michele Lessona, Ms Martina Gaia Baeli and Dr Emmanuele Parisi for their help in collecting data during the beamtimes. A big thanks also goes to Mr Hal Procacci for his help in lab, Mr Francesco Schimmenti and Mr Andrea Bezze for their help with the rheological analyses.

Appendix A. Supporting information

Supplementary data associated with this article can be found in the online version at doi:10.1016/j.foostr.2026.100568.

Data availability

Data available on Zenodo at DOI: 10.5281/zenodo.23057794

References

Abe, A. A., Aiello, I., Oliviero Rossi, C., & Caputo, P. (2025). Oleogels: Uses, applications, and potential in the food industry. In *Gels, 11*. Multidisciplinary Digital Publishing Institute (MDPI). https://doi.org/10.3390/gels11070563

Athukorala, Y., Mazza, G., & Dave Oomah, B. (2009). Extraction, purification and characterization of wax from flax (Linum usitatissimum) straw. *European Journal of Lipid Science and Technology, 111*(7), 705–714. https://doi.org/10.1002/ejlt.200800269

Bayomy, H. M., & Almasoudi, S. E. (2025). Physicochemical properties of oleogels based on sunflower or soybean oil structured with rice bran wax. *LWT, 238*. https://doi.org/10.1016/j.lwt.2025.118845

Blake, A. I., Co, E. D., & Marangoni, A. G. (2014). Structure and physical properties of plant wax crystal networks and their relationship to oil binding capacity. *Journal of the American Oil Chemists' Society, 91*(6), 885–903. https://doi.org/10.1007/s11746-014-2435-0

Brykczynski, H., Rudolph-Flöter, E. S. J., Schreiber, V., & Flöter, E. (2026). A novel, single-step LC-ELSD method to characterize the aliphatic fraction of natural waxes. *Food Chemistry, 510*. https://doi.org/10.1016/j.foodchem.2026.148570

Candela, D., Preston, J., Fiore, C., Parisi, E., Fraterrigo Garofalo, S., Demichelis, F., Fino, D., & Simone, E. (2025). Valorization of the lipid fraction of rice bran via supercritical CO2 and green solvent extraction processes. *Applied Food Research, 5*(2). https://doi.org/10.1016/j.afres.2025.101285

Cerqueira, M. A., Fasolin, L. H., Picone, C. S. F., Pastrana, L. M., Cunha, R. L., & Vicente, A. A. (2017). Structural and mechanical properties of organogels: Role of oil and gelator molecular structure. *Food Research International, 96*, 161–170. https://doi.org/10.1016/j.foodres.2017.03.021

Champagne Elaine, T. (Ed.). (2004). *Rice: Chemistry and technology*. American Association of Cereal Chemists.

Dassanayake, L. S. K., Kodali, D. R., & Ueno, S. (2011). Formation of oleogels based on edible lipid materials. *Current Opinion in Colloid and Interface Science, 16*(Number 5), 432–439. https://doi.org/10.1016/j.cocis.2011.05.005

Dassanayake, L. S. K., Kodali, D. R., Ueno, S., & Sato, K. (2009). Physical properties of rice bran wax in bulk and organogels. *JAOCS, Journal of the American Oil Chemists' Society, 86*(12), 1163–1173. https://doi.org/10.1007/s11746-009-1464-6

De Souza, R. J., Mente, A., Maroleanu, A., Cozma, A. I., Ha, V., Kishibe, T., Uleryk, E., Budylowski, P., Schünemann, H., Beyene, J., & Anand, S. S. (2015). Intake of saturated and trans unsaturated fatty acids and risk of all cause mortality, cardiovascular disease, and type 2 diabetes: Systematic review and meta-analysis of observational studies. In *BMJ (Online), 351*. BMJ Publishing Group. https://doi.org/10.1136/bmj.h3978

Dimakopoulou-Papazoglou, D., Zampouni, K., & Katsanidis, E. (2025). Natural waxes as gelators in edible structured oil systems: A review. In *Gels, 11*. Multidisciplinary Digital Publishing Institute (MDPI). https://doi.org/10.3390/gels11080656

Doan, C. D., Tavernier, I., Okuro, P. K., & Dewettinck, K. (2018). Internal and external factors affecting the crystallization, gelation and applicability of wax-based oleogels in food industry. In *Innovative Food Science and Emerging Technologies, 45* pp. 42–52). Elsevier Ltd. https://doi.org/10.1016/j.ifset.2017.09.023

Doan, C. D., Tavernier, I., Sintang, M. D. Bin, Danthine, S., Van de Walle, D., Rimaux, T., & Dewettinck, K. (2017). Crystallization and gelation behavior of low- and high melting waxes in rice bran oil: A case-study on berry wax and sunflower wax. *Food Biophysics, 12*(1), 97–108. https://doi.org/10.1007/s11483-016-9467-y

Doan, C. D., To, C. M., De Vrieze, M., Lynen, F., Danthine, S., Brown, A., Dewettinck, K., & Patel, A. R. (2017). Chemical profiling of the major components in natural waxes to elucidate their role in liquid oil structuring. *Food Chemistry, 214*, 717–725. https://doi.org/10.1016/J.FOODCHEM.2016.07.123

Doan, C. D., Van De Walle, D., Dewettinck, K., & Patel, A. R. (2015). Evaluating the oil-gelling properties of natural waxes in rice bran oil: Rheological, thermal, and microstructural study. *JAOCS, Journal of the American Oil Chemists' Society, 92*(6), 801–811. https://doi.org/10.1007/s11746-015-2645-0

Esposito, B., Sessa, M. R., Sica, D., & Malandrino, O. (2020). Towards circular economy in the agri-food sector. A systematic literature review. In *Sustainability (Switzerland), 12*. MDPI. https://doi.org/10.3390/SU12187401

Flores-García, C. L., Medina-Herrera, N., Rodríguez-Romero, B. A., Martínez-Ávila, G. C. G., Rojas, R., & Meza-Carranco, Z. (2023). Impact of fat replacement by using organic-candelilla-wax-based oleogels on the physicochemical and sensorial properties of a model cookie. *Gels, 9*(8). https://doi.org/10.3390/gels9080636

Gopala Krishna, A. G., Hemakumar, K. H., & Khatoon, S. (2006). Study on the composition of rice bran oil and its higher free fatty acids value. *JAOCS, Journal of the American Oil Chemists' Society, 83*(2), 117–120. https://doi.org/10.1007/s11746-006-1183-1

Hargrove, J. L., Greenspan, P., & Hartlet, D. K. (2004). Nutritional significance and metabolism of very long chain fatty alcohols and acids from dietary waxes. *Experimental Biology and Medicine, 229*.

Holey, S. A., Sekhar, K. P. C., Mishra, S. S., Kanjilal, S., & Nayak, R. R. (2021). Effect of oil unsaturation and wax composition on stability, properties and food applicability of oleogels. *Journal of the American Oil Chemists' Society, 98*(12), 1189–1203. https://doi.org/10.1002/aocs.12536

Hull, S. C., Mszar, R., Ostfeld, R. J., Ferrucci, L. M., Mucci, L. A., Giovannucci, E., & Loeb, S. (2025). Diet and prevention of cardiovascular disease and cancer. In *JACC: CardioOncology, 7* pp. 649–667). Elsevier Inc. https://doi.org/10.1016/j.jaccao.2025.07.008

Kavya, M., Udayarajan, C., Fabra, M. J., López-Rubio, A., & Nisha, P. (2024). Edible oleogels based on high molecular weight oleogelators and its prospects in food applications. *Critical Reviews in Food Science and Nutrition, 64*(13), 4432–4455. https://doi.org/10.1080/10408398.2022.2142195

Korhonen, J., Honkasalo, A., & Seppälä, J. (2018). Circular economy: The concept and its limitations. *Ecological Economics, 143*, 37–46. https://doi.org/10.1016/J.ECOLECON.2017.06.041

Loiacono, M., Padovano, L., Malacarne, M. C., Conti, S., & Caruso, E. (2025). Formulation and evaluation of alternative to beeswax for vegan lipsticks. *International Journal of Cosmetic Science, 47*(4), 626–638. https://doi.org/10.1111/ics.13060

Martins, A. J., Cerqueira, F., Vicente, A. A., Cunha, R. L., Pastrana, L. M., & Cerqueira, M. A. (2022). Gelation behavior and stability of multicomponent sterol-based oleogels. *Gels, 8*(1). https://doi.org/10.3390/gels8010037

Miyazawa, T., Tazawa, H., & Fujino, Y. (1978). Molecular species of triglyceride in rice bran. *Cereal Chemistry, 2*, 138–145.

Okuro, P. K., Tavernier, I., Bin Sintang, M. D., Skirtach, A. G., Vicente, A. A., Dewettinck, K., & Cunha, R. L. (2018). Synergistic interactions between lecithin and fruit wax in oleogel formation. *Food & Function, 9*(3), 1755–1767. https://doi.org/10.1039/C7FO01775H

Pandolsook, S., & Kupongsak, S. (2020). Potential use of policosanol extract from Thai bleached rice bran wax as an organogelator. *Journal of Food Measurement and Characterization, 14*(4), 2078–2086. https://doi.org/10.1007/s11694-020-00455-8

Principato, L., Carullo, D., Bassani, A., Spigno, G., Gruppi, A., Duserm Garrido, G., & Dordoni, R. (2021). Effect of dietary fiber and thermal conditions on rice bran wax-based structured edible oils. *Foods, 10*(12). https://doi.org/10.3390/foods10123072

Sahu, S., Ghosh, M., & Bhattacharyya, D. K. (2020). Utilization of unsaponifiable matter from rice bran oil fatty acid distillate for preparing an antioxidant-rich oleogel and evaluation of its properties. *Grasas York Aceites, 71*(1). https://doi.org/10.3989/gya.0938182

Samuditha, L., Dassanayake, K., Kodali, D. R., Ueno, S., & Sato, K. (2012). Crystallization kinetics of organogels prepared by rice bran wax and vegetable oils. *Journal of Oleo Science, 61*(Number 1). http://www.jstage.jst.go.jp/browse/jos/http://mc.manuscriptcentral.com/jjocs.

Scharfe, M., & Flöter, E. (2020). Oleogelation: From scientific feasibility to applicability in food products. In *European Journal of Lipid Science and Technology, 122*. Wiley-VCH Verlag. https://doi.org/10.1002/ejlt.202000213

Schnabel, L., Buscail, C., Sabate, J. M., Bouchoucha, M., Kesse-Guyot, E., Allès, B., Touvier, M., Monteiro, C. A., Hercberg, S., Benamouzig, R., & Julia, C. (2018). Association between ultra-processed food consumption and functional gastrointestinal disorders: Results from the french nutrinet-santé cohort. *American Journal of Gastroenterology, 113*(8), 1217–1228. https://doi.org/10.1038/s41395-018-0137-1

Shi, Y., Liu, C., Zheng, Z., Chai, X., Han, W., & Liu, Y. (2021). Gelation behavior and crystal network of natural waxes and corresponding binary blends in high-oleic sunflower oil. *Journal of Food Science, 86*(9), 3987–4000. https://doi.org/10.1111/1750-3841.15840

Sivakanthan, S., Fawzia, S., Madhujith, T., & Karim, A. (2022). Synergistic effects of oleogelators in tailoring the properties of oleogels: A review. In *Comprehensive reviews in food science and food safety, 21* pp. 3507–3539). John Wiley and Sons Inc. https://doi.org/10.1111/1541-4337.12966

Socrates, G. (2010). *Infrared and Raman characteristic group frequencies: tables and charts*. https://api.semanticscholar.org/CorpusID:92333066.

Springmann, M., Wiebe, K., Mason-D'croz, D., Sulser, T.B., Rayner, M., & Scarborough, P. (2018). *Health and nutritional aspects of sustainable diet strategies and their association with environmental impacts: a global modelling analysis with country-level detail*. www.thelancet.com/.

Stepanenko, D. (2025). The impact of ultra-processed foods on the risk of developing chronic diseases. *Universal Library of Medical and Health Sciences, 03*(02), 72–78. https://doi.org/10.70315/uloap.ulmhs.2025.0302012

Tan, T. H., Chan, E. S., Manja, M., Tang, T. K., Phuah, E. T., & Lee, Y. Y. (2023). Production, health implications and applications of oleogels as fat replacer in food system: A review. In *JAOCS, Journal of the American Oil Chemists' Society, 100* pp. 681–697). John Wiley and Sons Inc. https://doi.org/10.1002/aocs.12720

Tavernier, I., Doan, C. D., Van De Walle, D., Danthine, S., Rimaux, T., & Dewettinck, K. (2017). Sequential crystallization of high and low melting waxes to improve oil structuring in wax-based oleogels. *RSC Advances, 7*(20), 12113–12125. https://doi.org/10.1039/c6ra27650d

Thakur, D., Singh, A., Suhag, R., Dhiman, A., & Chauhan, D. S. (2023). Oleogelation based on plant waxes: Characterization and food applications. In *Journal of food science and technology, 60* pp. 2927–2944). Springer. https://doi.org/10.1007/s13197-023-05786-0

Toro-Vazquez, J. F., Morales-Rueda, J. A., Dibildox-Alvarado, E., Charó-Alonso, M., Alonzo-Macias, M., & González-Chávez, M. M. (2007). Thermal and textural properties of organogels developed by candelilla wax in safflower oil. *JAOCS, Journal of the American Oil Chemists' Society, 84*(11), 989–1000. https://doi.org/10.1007/s11746-007-1139-0

Vali, S. R., Ju, Y., Kaimal, T. N. B., & Chern, Y. (2005). A process for the preparation of food-grade rice bran wax and the determination of its composition. *Journal of the American Oil Chemists' Society, 82*(1), 57–64. https://doi.org/10.1007/s11746-005-1043-z

Wang, N., Chen, J., Zhou, Q., Jiang, L., Wang, L., Dai, Y., Yu, D., & Elfalleh, W. (2021). Crude wax extracted from rice bran oil improves oleogel properties and oxidative stability. *European Journal of Lipid Science and Technology, 123*(6). https://doi.org/10.1002/ejlt.202000091

Wang, P., Song, M., Eliassen, A. H., Wang, M., Fung, T. T., Clinton, S. K., Rimm, E. B., Hu, F. B., Willett, W. C., Tabung, F. K., & Giovannucci, E. L. (2023). Optimal dietary patterns for prevention of chronic disease. *Nature Medicine, 29*(3), 719–728. https://doi.org/10.1038/s41591-023-02235-5

Wang, Z., Chandrapala, J., Truong, T., & Farahnaky, A. (2023). Oleogels prepared with low molecular weight gelators: Texture, rheology and sensory properties, a review. In *Critical reviews in food science and nutrition, 63* pp. 6069–6113). Taylor and Francis Ltd. https://doi.org/10.1080/10408398.2022.2027339

Webb, P., Livingston Staffier, K., Lee, H., Howell, B., Battaglia, K., Bell, B. M., Matteson, J., McKeown, N. M., Cash, S. B., Zhang, F. F., Decker Sparks, J. L., & Blackstone, N. T. (2023). Measurement of diets that are healthy, environmentally sustainable, affordable, and equitable: A scoping review of metrics, findings, and research gaps. In *Frontiers in nutrition, 10*. Frontiers Media S.A. https://doi.org/10.3389/fnut.2023.1125955

Wettlaufer, T., Brykczynski, H., & Flöter, E. (2021). Wax-based oleogels—Properties in medium chain triglycerides and canola oil. *European Journal of Lipid Science and Technology, 124*(2). https://doi.org/10.1002/ejlt.202100114

Wijarnprecha, K., Aryusuk, K., Santiwattana, P., Sonwai, S., & Rousseau, D. (2018). Structure and rheology of oleogels made from rice bran wax and rice bran oil. *Food Research International, 112*, 199–208. https://doi.org/10.1016/j.foodres.2018.06.005

Zhang, Y., Xu, J., Tang, C., & Li, Y. (2023). *Crystallization behavior and physical properties of monoglycerides-based oleogels as function of oleogelator concentration.* https://doi.org/10.3390/foods.